The Complexity of the Complexes. A Twelve-fold Anchored Ligand in a Co(II) Hybrid Polymeric Material with Ferromagnetic Order

N. Snejko, E. Gutiérrez-Puebla, J. L. Martínez, M. A. Monge,* and C. Ruiz-Valero

Instituto de Ciencia de Materiales de Madrid, CSIC, Cantoblanco, 28049 Madrid, Spain

Received November 26, 2001

Single crystals of the new organo-inorganic polymer $Co_2[O_8C_{10}H_2]$ were hydrothermally obtained. Conditions for the synthesis are reported. The crystal structure of this material was established by single-crystal X-ray diffraction: monoclinic, space group $C2/m$, a = 6.161(1) Å, b = 17.478(4) Å, c = 4.554(1) Å, β = 115.735(4)°. The 3D structure can be envisaged in terms of edge-sharing CoO_6 octahedra chains running along the [100] direction kept together in the [001] direction through the carboxylate groups and in the [010] direction through the multidentate benzene-1,2,4,5,-tetracarboxylate ligand. In this organo-inorganic hybrid compound, the ligand coordinates to 12 different cobalt atoms. This kind of coordination forces the formation of 1D chains in which the Co atoms are very close to each other and confers on the material interesting magnetic properties. Long-range 3D ferromagnetic order is obtained at T_C = 14.9 K, with a saturation magnetization of 4.3 μ_B/formula unit and H_C = 2.2 kOe.

Introduction

The rapidly expanding field of crystal engineering of infinite 2D- and 3D-coordinated polymers is of great current interest for both the structural and topological novelty of such organic−inorganic frameworks, as well as for their potential application as functional materials. Magnetism, electrical conductivity, and the possibility of application in gas separation or heterogeneous catalysis are among other distinguishing features of these promising materials.[1−8]

Intense research activities in this field have recently produced very diverse new metal−organic polymers.[9−13] The main strategy widely used in this area is a building-block approach. Usually, bi- or multidentate ligands containing N or O donors with more or less rigid conformations function as connectors by binding the metal centers. The versatility of organic functional groups and the diversity of metal coordination geometries have led to a wide array of complex organo-inorganic polymeric structures. In this way, symmetric molecular organic building blocks can be copolymerized with transition metal ions to give hybrid polymers. It is worth mentioning that polycarboxylic acids, particularly some highly symmetric ones, as the benzene-di- and tricarboxylic acids, in reactions with different metal ions have yielded a wide variety of fascinating moderately robust open-framework architectures having unusual properties.[14,15] Specifically, benzen-1,4-dicarboxylic, benzene-1,3,5-tricarboxylic, 1,3,5-cyclohexanetricarboxylic acids, etc., have been largely used to give one-, two-, and three-dimensional porous networks[16−18] exploiting both the diversity of metal coordination geometries and the weak intermolecular forces such as $\pi-\pi$ interactions and hydrogen bonding. In this sense, benzene-1,2,4,5,-tetracarboxylic acid (H_4BTEC) seems to be a promising ligand, providing a building block of high symmetry, with charge and multi-connecting ability, that has not, to our knowledge, been applied as the only connector in the design of coordination polymers. We describe here the synthesis, crystal structure, ther-

* To whom correspondence should be addressed. E-mail: amonge@icmm.csic.es. Fax: (34) 91-3720623.

(1) Subramanian, S.; Zaworotko, M. J. *Coord. Chem. Rev.* **1994**, *137*, 357.
(2) Batten, S. R.; Robson, R. *Angew. Chem., Int. Ed.* **1998**, *37*, 1460.
(3) Miller, J. S. *Adv. Mater.* **2001**, *13*, 525.
(4) Chen, B.; Eddaoudi, M.; Hyde, S. T.; O'Keeffe, M.; Yaghi, O. M. *Science* **2001**, 1021.
(5) Plater, M. J.; Foreman, M. R. St. J.; Coronado, E.; Gómez-García, C. J.; Slawin, A. M. Z. *J. Chem. Soc., Dalton Trans.* **1999**, 4209.
(6) Robson, R. *J. Chem. Soc., Dalton Trans.* **2000**, 3735.
(7) Zhang, H.; Wang, X.; Zhang, K.; Teo, B. K. *J. Solid State Chem.* **2000**, *152*, 191.
(8) Hagrman, P. J.; Hagrman, D.; Zubieta, J. *Angew. Chem., Int. Ed.* **1999**, *38*, 2638.
(9) See, for example: Bowes, C. L.; Ozin, G. A. *Adv. Mater.* **1996**, *8*, 13. Coronado, E.; Galán-Mascarós, J. R.; Gómez-García, C. J. *J. Chem. Soc., Dalton Trans.* **2000**, 205.
(10) Gutschke, S. O. H.; Price, D. J.; Powell, A. K.; Wood, P. T. *Angew. Chem., Int. Ed.* **2001**, *40*, 1920.
(11) Price, D. J.; Powell, A. K.; Wood, P. T. *Dalton Trans.* **2000**, *20*, 3566.
(12) Choudhury, A.; Natarajan, S.; Rao, C. N. R. *J. Solid State Chem.* **2000**, *155*, 62.
(13) Ekambaram, S.; Sevov, S. C. *J. Mater. Chem.* **2000**, *10*, 2522.
(14) Kepert, C. J.; Prior, T. J.; Rosseinsky, M. J. *J. Solid State Chem.* **2000**, *152*, 261.
(15) Moulton, B.; Lu, J.; Mondal, A.; Zaworotko, M. J. *J. Chem. Soc., Dalton Trans.* **2001**, 863.
(16) Eddaudi, H.; Li, H. L.; Yaghi, O. M. *J. Am. Chem. Soc.* **2000**, *122*, 1391.
(17) Chui, S. S. Y.; Lo, S. M. F.; Charmant, J. P. H.; Orpen, A. G.; Williams, I. D. *Science* **1999**, *283*, 1148.
(18) Kumagai, H.; Akita-Tanaka, M.; Inoue, K.; Kurmoo, M. *J. Mater. Chem.* **2001**, Advance Article.

10.1021/cm011286p CCC: $22.00
Published on Web 03/28/2002

Table 1. Crystal Data and Structure Refinement for Co_2[BTEC]

empirical formula	$Co_2[O_8C_{10}H_2]$
formula weight	367.98
temperature	296(2) K
wavelength	0.71073 Å
crystal system	monoclinic
space group	*C*2/*m*
unit cell dimensions	$a = 6.161(1)$ Å $b = 17.478(4)$ Å $\beta = 115.735(4)°$ $c = 4.554(1)$ Å
volume, *Z*	441.7(2) Å^3, 2
density (calculated)	2.767 Mg/m^3
absorption coefficient	3.802 mm^{-1}
F(000)	360
crystal size	0.25 mm × 0.25 mm × 0.20 mm
Θ range for data collection	3.85−31.18°
limiting indices	(−8, −24, −6) (5, 25, 6)
reflections collected	1639
independent reflections	686 ($R_{int} = 0.052$)
absorption correction	sadabs
max and min transmission	1.43 and 0.79
refinement method	full-matrix least-squares on F^2
data/restraints/parameters	686/0/51
goodness-of-fit on F^2	1.036
final *R* indices [$I > 2\sigma(I)$]	R1 = 0.046, wR2 = 0.099
R indices (all data)	R1 = 0.067, wR2 = 0.105
largest diff peak and hole	0.869 and −1.179 eÅ^{-3}

mogravimetic analysis, and IR and magnetic properties of the coordination polymer Co_2(BTEC).

Experimental Section

General Information. $CoCL_2 \cdot 6H_2O$, H_4BTEC, and Et_3N were obatined from Aldrich. C and H analysis was carried out with a Heraeus apparatus. Thermogravimetric and differential thermal analysis (TGA-DTA) was performed on a Seiko TG/DTA 320 apparatus in both flowing dinitrogen and air atmospheres, at a heating rate of 5 °C cm^{-1} in the temperature range between 25 and 700 °C.

Synthesis. The compound was synthesized from a reaction mixture containing $CoCl_2 \cdot 6H_2O$, $O_8C_{10}H_2$ (H_4BTEC), Et_3N, and H_2O in a molar ratio of 2:1:5:80 under hydrothermal conditions. The mixture was heated at 180 °C for 5 days. The resulting dark violet crystals were filtered and washed thoroughly with deionized water and ether. Elemental analysis calculated for $Co_2C_{10}H_2O_8$: C, 32.61%; H, 0.54%. Found: C, 32.07%; H, 0.47%.

X-ray Structure Determination. Data for a dark violet crystal of $Co_2[O_8C_{10}H_2]$ were collected in a Siemens SMART-CCD diffractometer, over a hemisphere of reciprocal space by a combination of three exposures. Each exposure of 20 s covered 0.3° in ω. Unit cell dimensions were determined by a least-squares fit of 60 reflections with $I > 20\sigma(I)$. Data were collected using an ω scan over the range $3 < \theta < 31°$. The total number of reflections measured was 1639, of which 686 were independent. The structure was solved by direct methods. Refinement was carried out by full-matrix least-squares analysis with anisotropic thermal parameters for all atoms. Hydrogen atoms were located in a Fourier map and isotropically refined. The final residuals were $R_F = 0.046$ for $I > 2\sigma(I)$ and 0.066 for all data. A summary of the fundamental crystal and refinement data is given in Table 1. Most of the calculations were carried out with SMART software for data collection and data reduction and SHELXTL.[19]

Magnetic Measurements. dc magnetic measurements were carried out using a SQUID (Quantum Design) magnetometer operating from 350 to 1.8 K at different magnetic fields up to 50 kOe. ac susceptibility was measured in a frequency range from 0.3 Hz to 1 kHz, with a field amplitude of 1Oe.

(19) *Software for the SMART™ System V5.04 and SHELXTL™ V5.1*; Bruker-Siemens Analytical X-ray Instrument Inc.: Madison, WI, 1998.

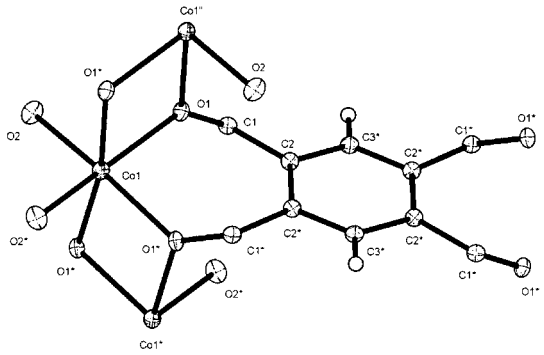

Figure 1. Labeled ORTEP plot of the building unit in the hybrid polymer Co_2[BTEC] showing more than the asymmetric unit. * indicates atoms that are symmetrically related.

Table 2. Atomic Coordinates and Equivalent Isotropic Displacement Parameters for Co_2[BTEC]

atom	*X*	*Y*	*Z*	Ueq[a]
Co1	0.0000	0.2897(1)	0.0000	11(1)
O1	0.2607(5)	0.3004(1)	−0.2105(6)	12(1)
O2	0.2047(5)	0.3659(2)	0.3424(6)	14(1)
C1	0.2881(7)	0.3597(2)	−0.3530(9)	10(1)
C2	0.4080(7)	0.4301(2)	−0.1618(8)	10(1)
C3	0.3252(9)	0.5000	−0.312 (1)	10(1)

[a] Ueq ($\times 10^3$ Å^2) is defined as one-third of the trace of the orthogonalized *Uij* tensor.

Specific heat measurements were performed with a quasi-adiabatic relaxation technique in a temperature range from 1.8 to 200 K. The sample in the form of pellets was mounted on a small alumina plate with a small amount of Apiezon grease for a better thermal contact.

Results and Discussion

The crystallization process in hydrothermal synthesis is of a nonequilibrium nature, and despite the simplicity of the procedure, any small change in any reaction condition (pH, temperature, time, etc.) affects the reaction outcome. Many factors had to be tuned to reach the desired coordination of the previously selected benzene-1,2,4,5,-tetracarboxylate ligand (H_4BTEC). Finally, under the above indicated conditions, a violet crystalline product was obtained.

X-ray single-crystal studies on a sample obtained from the reaction products revealed a composition of $Co_2[O_8C_{10}H_2]$ and an extended framework structure composed of the building units shown in Figure 1. In the asymmetric unit, there is one only Co atom, situated on the 2-fold axis, and one-quarter of the $(BTEC)^{4-}$ counterion. The Co atom exhibits a quite distorted octahedral coordination, with the apical distances [2.208(3) Å] being longer than the equatorial ones [d_{av} = 2.052(3) Å] (see Tables 2 and 3). Although the Jahn−Teller distortion for a Co^{2+} cation in a $t_{2g}^5e_g^2$ high-spin configuration is rarely observed, in this compound, this effect is strengthened by the peculiar coordination of the chelating ligand and solid-state packing effects. Of the two oxygen atoms in each carboxylate group, one (O1) is bonded in a bifurcated way to two different Co atoms, giving rise to chains of Co doubly bridged by oxygen atoms. The other (O2) coordinates in the usual manner and establishes cohesion among different Co rows. The structure can be envisaged in terms of edge-sharing CoO_6 octahedra chains running along the [100] direc-

Table 3. Selected Bond Lengths (Å) and Angles (°) for Co_2[BTEC]

bond or angle[a]		bond or angle[a]	
Co1−O2	2.022(3)	Co1−O2[1]	2.022(3)
Co1−O1[2]	2.084(3)	Co1−O1[3]	2.083(3)
Co1−O1	2.207(3)	Co1−O1	2.207(3)
O1−C1	1.273(4)	O1−Co1[3]	2.084(3)
O1−C2[4]	1.258(4)	C1−O2[5]	1.258(4)
C1−C2	1.503(5)	C2−C3	1.385(4)
C2−C2[6]	1.416(7)	C3−C2[7]	1.385(4)
O2−Co1 −O2[1]	97.6(2)	O2−Co1−O1[2]	158.8(1)
O2[1]−Co1−O1[2]	93.6(1)	O2−Co1−O1[3]	93.6(1)
O2[1]−Co1−O1[3]	158.9(1)	O1[2]−Co1−O1[3]	81.9(2)
O2−Co1−O1[1]	86.4(1)	O2[1]−Co1−O1[1]	87.2(1)
O1[2]−Co1−O1[1]	76.2(1)	O1[3]−Co1−O1[1]	111.5(1)
O2−Co1−O1	87.2(1)	O2[1]−Co1−O1	86.4(1)
O1−Co1−O1	111.5(1)	O1[3]−Co1−O1	76.2(1)
O1[1]−Co1−O1	170.3(1)	C1−O1−Co1[3]	128.8(2)
C1−O1−Co1	124.9(2)	Co1[3]−O1−Co1	103.9(1)
C1[4]−O2−Co1	127.8(3)	O2[5]−C1−O1	123.5(3)

[a] Symmetry transformations used to generate equivalent atoms: 1 = ($-x$, y, $-z$), 2 = ($x - {}^1/_2$, $-y + {}^1/_2$, z), 3 = ($-x + {}^1/_2$, $-y + {}^1/_2$, z), 4 = (x, y, $z + 1$), 5 = (x, y, $z - 1$), 6= ($-x + 1$, y, $-z$), 7 = (x, $-y + 1$, z).

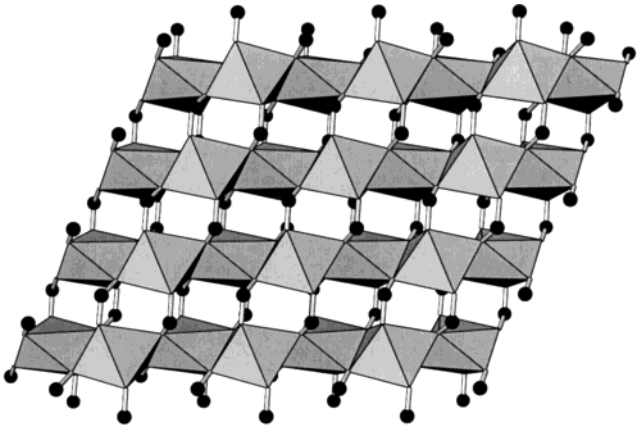

Figure 2. View along the [010] direction of the CoO_6 edge-sharing polyhedra chains and the connectivity among them through the carboxylate groups.

tion, kept together in the [001] direction through the carboxylate groups. This arrangement generates pseudo-layers parallel to the *ac* plane, in which the Co−Co distances are 3.37 and 4.55 Å for atoms from the same chain and between chains, respectively (Figure 2). The octahedra are tilted with respect to one another because of the three bonds to cobalt of each carboxylate group, the angles Co−O−Co and Co−Co−Co being 103.9 and 131.5°, respectively.

The layers, which are pillared perpendicularly to the [010] direction, are bridged in this direction by the $(BTEC)^{4-}$ counterions, giving rise to a rigid octahedral polymer (Figure 3). There are two different distances among Co atoms belonging to contiguous layers, 7.35 and 10.12 Å, which alternate along the *b* direction as a consequence of the tilting of the chains. The aromatic rings are aligned along the [102] direction, thus minimizing the $\pi-\pi$ interaction (Figure 4). The distance between the ring centroids is 4.55 Å. The multiple coordination of the ligand to different Co atoms favors short distances between them but prevents the formation of large tunnels in this structure. Although there is a tridimensional net of small channels, these channels are mostly occupied by the hydrogen atoms of the aromatic rings.

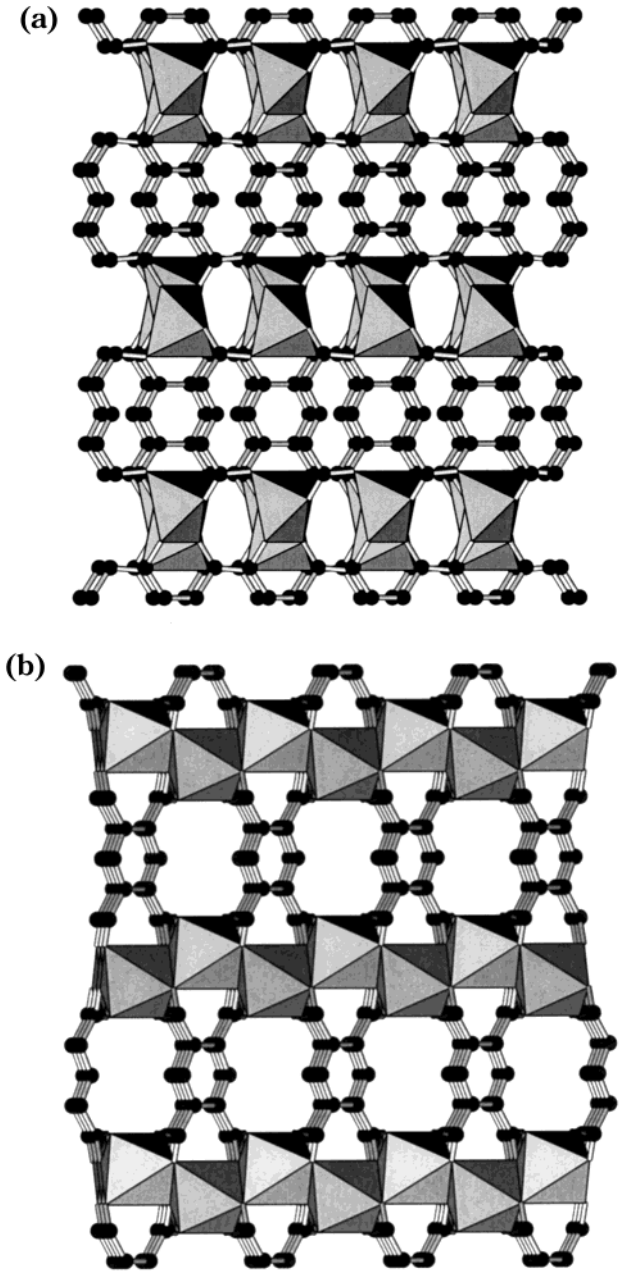

Figure 3. View of the 3D structure of Co_2[BTEC] (a) along the [100] direction and (b) along the [101] direction.

The thermogravimetric analysis showed thermal stability for the compound up to 400 °C in N_2 and up to 350 °C in air. Further heating resulted in Co_3O_4 (calculated 43.6%, found 43.0%), as indicated by powder X-ray diffraction. In the infrared spectrum of the compound, the antisymmetric $\nu_{asym}(OCO^-)$ vibrations appear in the range 1484−1556 cm[1], the bands corresponding to the symmetric $\nu_{sym}(OCO^-)$ vibrations being found in the 1350−1395 cm^{-1} range. This relative positioning of the antisymmetric and symmetric vibration bands[20] agrees with the bridging character of the carboxylate groups in the structure.

Magnetic analysis (Figure 5) shows the magnetic susceptibility for an applied magnetic field of 3.5 kOe. The inverse susceptibility shows almost perfectly linear

(20) Nakamoto, K. *Infrared and Raman Spectra of Inorganic and Coordination Compounds*; John Wiley: New York, 1986.

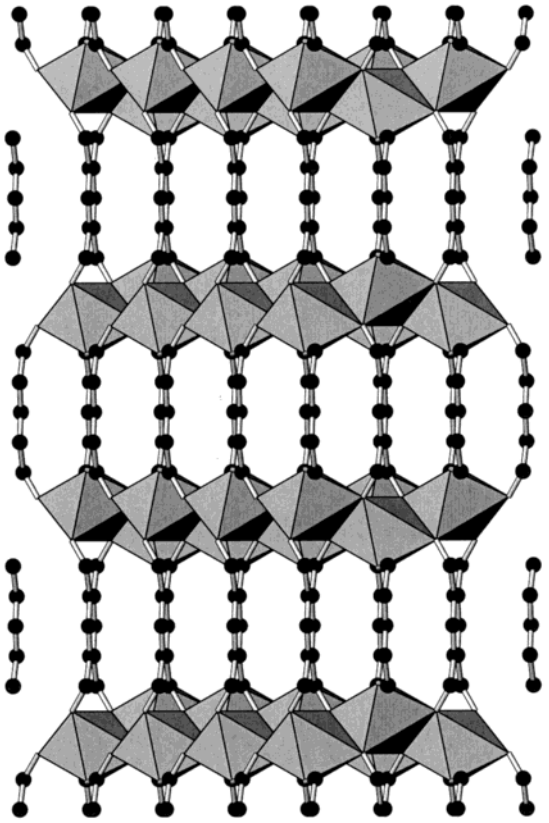

Figure 4. View of the aromatic rings aligned along the [102] directions.

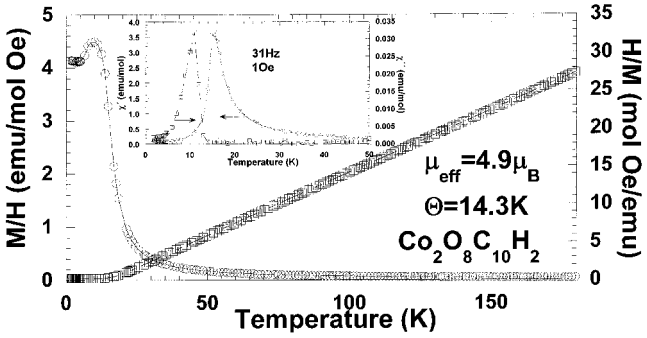

Figure 5. Temperature dependence of the magnetic susceptibility and of the inverse susceptibility at 3.5 kOe. The inset shows the ac susceptibility at 31 Hz and 1 Oe.

Curie−Weiss behavior from 30 to 200 K, with an effective paramagnetic moment of 4.9μ_B/Co and a Weiss constant of +14.3 K, indicating dominant ferromagnetic interactions between adjacent Co^{2+} ions. The inset shows the ac magnetic susceptibility measured at 31 Hz. The real part of the susceptibility display a clear peak at 14.9 K, independent of the applied frequency, indicating long-range ferromagnetic order with T_C = 14.9 K. However, the imaginary part shows a much weaker peak centered at 11 K. This effect is often observed in molecular magnets.[21,22]

The isothermal magnetization was measured at different temperatures (close to T_C) and magnetic fields

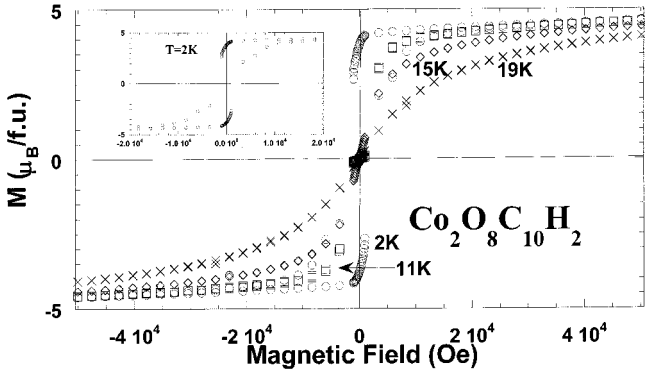

Figure 6. Hysteresis loops up to 50 kOe, measured at different temperatures around T_C. The inset shows the low-field part of the hysteresis loops at 2 K.

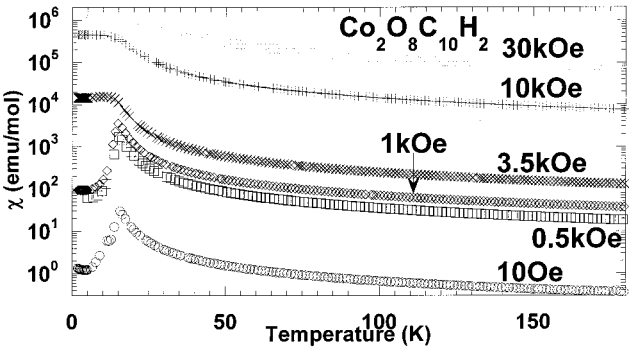

Figure 7. Temperature dependence of the magnetic dc susceptibility at different magnetic fields between 10 Oe and 30 kOe.

up to 50 kOe, as presented in Figure 6. Above 15 K, the magnetization is almost linear, as expected from a paramagnetic system. At low temperature (2 K), the hysteresis loop is close to that of a ferromagnet, with a coercive field of H_C = 2kOe and a saturation magnetization of $M_S = 4.3\mu_B$/formula unit These values are again expected for Co^{2+} ions ferromagnetically ordered in a octahedral environment.

Figure 7 shows the temperature dependence of the dc magnetic susceptibility measured at different applied magnetic fields in the range from 10 Oe to 30 kOe (after zero-field cooling). For low fields (H < 2 kOe < H_C), the magnetic susceptibility shows a clear cusp at 14.9 K that could be interpreted as antiferromagnetic ordering or a reduction in susceptibility due to the formation of randomly oriented ferromagnetic domains. For higher fields, the susceptibility is clearly saturated at temperatures below T_C, as expected for a ferromagnet. To check this field dependence of the susceptibility, we fixed the temperature close to T_C = 14.9 K and measured the ac magnetic susceptibility for different dc magnetic fields around H_C. Figure 8 shows the isothermal ac susceptibility multiplied by the applied magnetic field as a function of the applied field and the alternating frequency. The susceptibility strongly increases for low fields up to H_C = 2.2 kOe. For higher magnetic fields, the ac susceptibility is almost constant or decreasesslightly. These data are in qualitative agreement with the dc susceptibility measurements presented in Figure 7.

From the magnetic and structural data, a more plausible explanation is that Co^{2+} cations along the

(21) Coronado, E.; Galán-Mascarós, J. R.; Gómez-García, C. J.; Martínez-Agudo, J. M.; Martínez Ferroso, E.; Waerenborgh, J. C.; Almeida, M. *J. Solid State Chem.* **2001**, *159*, 391.

(22) Kurmoo, M.; Kumagai, H.; Green, M. A.; Lovett, B. W.; Blundell, S. J.; Ardavan, A.; Singleton, J. *J. Solid State Chem.* **2001**, *159*, 343.

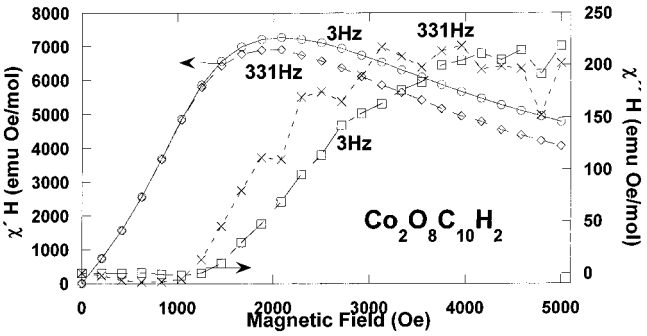

Figure 8. Field dependence of the real and imaginary parts of the ac susceptibility multiplied by the applied magnetic field at 2 frequencies (3 and 331 Hz).

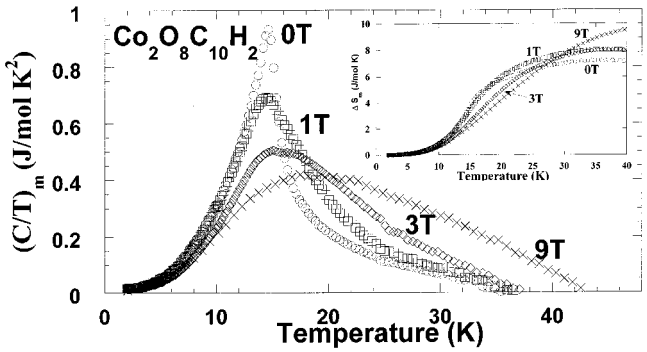

Figure 9. Temperature dependence of the magnetic specific heat divided by temperature at different applied magnetic fields. The inset shows the magnetic entropy as a function of temperature and field.

chain are ferromagnetically coupled, as expected from the Goodenough−Kanamori rules for a Co−O−Co exchange angle of 103.9°. These are the observed data extracted from the Curie−Weiss behavior of the magnetic susceptibility. Because of the short distances between adjacent chains, i.e., Co−Co distance of 4.55 Å, which is not far from the distance inside the chain (3.37 Å), we expect the coupling between chain to be ferromagnetic and long-range ferromagnetic order to be obtained at T_C = 14.9 K. Nevertheless, for magnetic fields lower than H_C, the system could present some reduced susceptibility, probably related to ferromagnetic domain formation and domain dynamics.

Specific heat measurements were performed up to 200 K under different applied magnetic fields on small pellets of syntherized $Co_2O_8C_{10}H_2$. A clear λ-type anomaly was observed close to T_C =14.9 K, indicating a magnetic transition, in agreement with the magnetic susceptibility data. To obtain the pure magnetic contribution to the specific heat, we have to subtract the lattice and electronic contributions to the total specific heat. In the low-temperature range (below 50−60 K), these two components depend on temperature in a linear and cubic fashion. The electronic component is expected to be very small because the system behaves as an insulator at room temperature. Figure 9 shows the temperature dependence of $(C/T)_m$, obtained after the proper subtraction of the electronic and lattice contributions, at different applied magnetic fields. The effect of the magnetic field is to smear out the sharp transition, distributing the total entropy over a wide temperature range. In the inset is shown the magnetic entropy as a function of the temperature obtained from the integration of the magnetic specific heat as $\int C_m/T\ dT$.

The expected value for Co^{2+} ($S = {}^3/_2$) is $R \ln 4 = 11.52$ J/(mol K). The experimental result for zero-field cooling is 63% of the expected value, and for a field of 9 T, it i almost 84% of the expected theoretical value. The anomaly at 14.9 K for 0 T is rather asymmetric with the shape of a rounded λ. This fact could indicate a first-order transition, but the quality of the data does not allow us to ensure the character of the transition.

In conclusion, by using a highly charged very symmetric ligand and adjusting the synthesis conditions, we were able to obtain an organic−inorganic hybrid compound in which the ligand coordinates to 12 different cobalt atoms. This kind of coordination forces the formation of 1D chains in which the Co atoms are very close to each other and drives the formation of a 3D hybrid structure with long-range ferromagnetic order.

Acknowledgment. This work was supported by the Spanish CICYT MAT1999-0892.

CM011286P